

Simultaneous measurement of humidity and temperature based on fiber-tip microcantilever cascaded with fiber Bragg grating

DAN LIU,^{1,2} ZHIHAO CAI,^{1,2} BOZHE LI,^{1,2} MENGQIANG ZOU,^{1,2}
LICHAO ZHANG,^{1,2} YUNZHI HUA,³ JUNHAO MAI,⁴ CONG ZHAO,^{4,†*}
CHANGRUI LIAO,^{1,2,5,†}  JUN HE,^{1,2}  XIAOYU WENG,¹  LIWEI
LIU,¹ JUNLE QU,¹ AND YIPING WANG^{1,2} 

¹Key Laboratory of Optoelectronic Devices and Systems of Ministry of Education and Guangdong Province, College of Physics and Optoelectronic Engineering, Shenzhen University, Shenzhen 518060, China

²Shenzhen Key Laboratory of Photonic Devices and Sensing Systems for Internet of Things, Guangdong and Hong Kong Joint Research Centre for Optical Fiber Sensors, Shenzhen University, Shenzhen 518060, China

³Shenzhen Institute of Information Technology, Shenzhen 518172, China

⁴Guangdong Laboratory of Artificial Intelligence and Digital Economy (SZ), Shenzhen 518107, China

⁵cliao@szu.edu.cn

†These authors contributed equally.

*zhacong@szu.edu.cn

Abstract: We demonstrated a hybrid sensor of fiber Bragg grating (FBG) and Fabry-Perot interferometer (FPI) based on fiber-tip microcantilever for simultaneous measurement of temperature and humidity. The FPI was developed using femtosecond (fs) laser-induced two-photon polymerization to print the polymer microcantilever at the end of a single-mode fiber, achieving a humidity sensitivity of 0.348 nm/%RH (40% to 90%, when temperature = 25 °C ± 0.1 °C), and a temperature sensitivity of -0.356 nm/°C (25 to 70 °C, when RH% = 40% ± 1%). The FBG was line-by-line inscribed in the fiber core by fs laser micromachining, with a temperature sensitivity of 0.012 nm/°C (25 to 70 °C, when RH% = 40% ± 1%). As the shift of FBG-peak on the reflection spectra is only sensitive to temperature rather than humidity, the ambient temperature can be directly measured by the FBG. The output of FBG can also be utilized as temperature compensation for FPI-based humidity measurement. Thus, the measured result of relative humidity can be decoupled from the total shift of FPI-dip, achieving the simultaneous measurement of humidity and temperature. Gaining the advantages of high sensitivity, compact size, easy packaging, and dual parameter measurement, this all-fiber sensing probe is anticipated to be applied as the key component for various applications involving the simultaneous measurement of temperature and humidity.

© 2023 Optica Publishing Group under the terms of the [Optica Open Access Publishing Agreement](#)

1. Introduction

The accurate measurement of humidity is of great significance for industrial and agricultural production, environmental monitoring, food safety and other fields [1]. Various types of commercialized electrical humidity sensors have been reported, such as resistive/capacitive sensors [2–4]. Although these electrical humidity sensor are with the advantages of high accuracy and fast response, they often involve in problems of poor long-term stability and interchangeability, and fail in some special applications (such as in strong electromagnetic environment) [5,6]. What's more, humidity change is usually associated with other parameters, such as temperature and pressure [7]. Simultaneous measurement of temperature and humidity is required in the applications of weather forecast, medical biology and food storage [8–10].

Fiber optic humidity sensor has the advantages of small size, light weight, immunity from electromagnetic interference, etc [4,11]. In recent years, there has been large number of reports about fiber optic humidity sensors [6,12]. Among them, the humidity sensor based on Fabry-Perot interferometer (FPI) has outstanding performance. FPI is an important optical fiber sensing technology, which has been widely used in physics, chemistry and biomedical sensing due to its compact size, easy manufacture, low cost and excellent stability [4,13,14].

Recently, our group have demonstrated a series of applications using a micro FPI on a fiber-tip for the measurement of nanoforce and hydrogen with high sensitivity and rapid response, respectively [15–17]. The fiber-tip micro FPI was fabricated by femtosecond (fs)-laser induced two-photon polymerization (TPP) technology, with the unique advantages of high precision, high flexibility, and true 3D processing capability, etc. Fs-laser induced TPP is basically a form of additive manufacturing, based on two-photon absorption (TPA) that two photons simultaneously transfer their energy to an absorbing molecule or material. Since the rate of TPA is proportional to the square of the light intensity, the polymerization can only occur at the center of the fs-laser focus point with high light intensity (\sim TW/cm²). Such nonlinear threshold effect allows the feature size of TPP to easily break the optical limit, currently down to 10 nm. Based on optimized fs-laser induced TPP technology for fabricating the fiber-tip FPI, we also have proposed an all-fiber wearable breath sensor based on FPI formed by fiber-tip microcantilever with ability to detect various types of breath patterns [18]. The fabricated sensor was also turned out to be with a high sensitivity to humidity, however suffered from the issue of cross sensitivity between temperature and humidity. Thus, to achieve an accurate humidity measurement, it is necessary to solve the cross-sensitivity issue.

In this letter, a simultaneous temperature and humidity measurement system based on fiber Bragg grating (FBG) and FPI is proposed. The FPI formed by the fiber-tip microcantilever and fiber end face was with high sensitivity to humidity change, however was also sensitive to the change of ambient temperature. Thus, an FBG which was only sensitive to temperature rather than humidity was introduced to compensate the response of FPI humidity sensor, so as to realize the purpose of dual parameter sensing of temperature and humidity, simultaneously. The hybrid sensor of FBG and FPI presented excellent sensitivity for humidity measurement as high as 0.348 nm/%RH, which turned out to be higher than that of the similar fiber sensors with cascaded structures.

2. Sensing principle

The schematic diagram of the hybrid sensor consisting of FBG and FPI based on fiber-tip microcantilever for simultaneous measurement of temperature and humidity is shown in Fig. 1. An FP cavity was formed by the suspended microcantilever and the end face of the fiber. Then an interference pattern can be induced by the three-beam interference by lights from the fiber end face, the lower and the upper surfaces of the microcantilever [10,12]. The relationship between the dip wavelength shift ($\Delta\lambda_r$) of the interference pattern and the FP cavity length reduction (ΔL) is

$$\Delta\lambda_r/\lambda_r = \Delta L/L \quad (1)$$

where, λ_r is the dip wavelength, and L is the FP cavity length.

As the microcantilever was printed by femtosecond (fs) laser-induced two-photon polymerization (TPP) using photoresist which was a polymer material, the geometries of the microcantilever could change as a result of swelling/shrinking induced by thermal and humidity (absorbing/exuding water molecules) effects. Thus, the FP cavity length could change as a result of altered microcantilever geometries and eventually induce the shift of dip wavelength in the reflection spectra of FPI. In other words, the wavelength shift of FPI-dip was due to the hybrid effect of temperature and humidity.

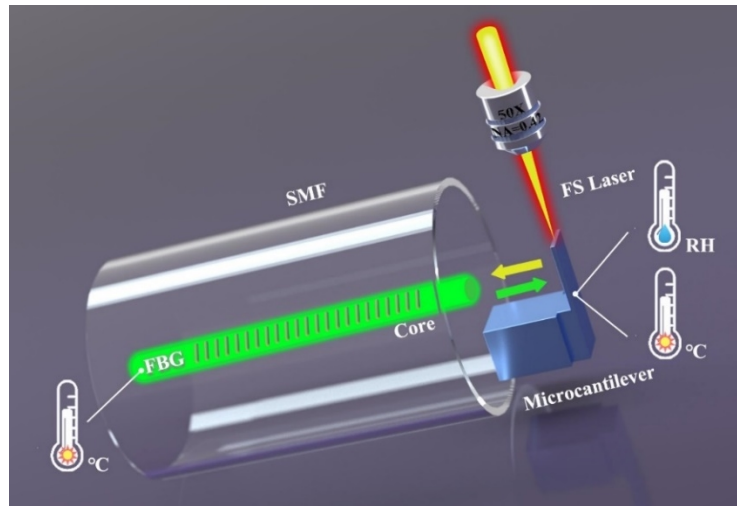


Fig. 1. Schematic diagram of the all-fiber sensor for simultaneously measuring humidity and temperature based on the fiber-tip microcantilever cascaded with FBG.

To reveal the temperature information and obtain the exact humidity value, an FBG was written into the fiber core in a line-by-line manner. The Bragg resonant wavelength center (λ_{FBG}) of the m th order FBG is given as [19,20]:

$$m\lambda_{FBG} = 2n_{eff}\Lambda \quad (2)$$

where n_{eff} is the effective refractive index (RI) of the core mode and Λ is the grating period.

The external perturbation on FBG (e.g., temperature change) can result in a shift of central wavelength, while the FBG in fiber is not sensitive to humidity as its working mode is confined in the core where the humidity induced RI change does not take effects. Thus, the shift of FBG center wavelength is only relevant to temperature change. Eventually, the exact humidity value can be obtained from the wavelength shift of FPI-dip together with the compensation from temperature information of the resonant wavelength shift of FBG.

3. Materials and methods

3.1. Device fabrication

The FBG was fabricated at the core by fs-laser micromachining with 100X objective lens (NA = 1.25), as shown in Fig. 2(a). The fs laser was with a wavelength of 1026 nm, a pulse repetition rate of 200 kHz, a pulse width of 250 fs, and an average power of 1.14 mw. The second order FBG was fabricated with a grating period of 1.070 μm and a total length of 300 μm in a single mode fiber (SMF), as shown in Fig. 2(c). The width of FBG was around 10 μm , which was slightly larger than the fiber core diameter, to ensure that the light could completely transmit through the FBG.

The fiber-tip microcantilever was subsequently fabricated by fs-laser induced TPP, as shown in Fig. 2(b), using a commercial negative photoresist (PR) (Zhichu Optics Co. Ltd., China). The PR is composed by a photo-initiator (IGR-369, from Ciba Specialty Chemicals, Switzerland), monomers (SR444, SR368 and SR454, from Sartomer, USA), a polymerization inhibitor (4-Hydroxyanisole, MEHQ, from Sigma Aldrich, USA) and an accelerator promoter (tetraethyl thiuram disulphide, TED, from Sigma Aldrich, USA). The fabrication process has been described in detail elsewhere [21]. Firstly, a precleaned SMF was mounted in between a glass slide and

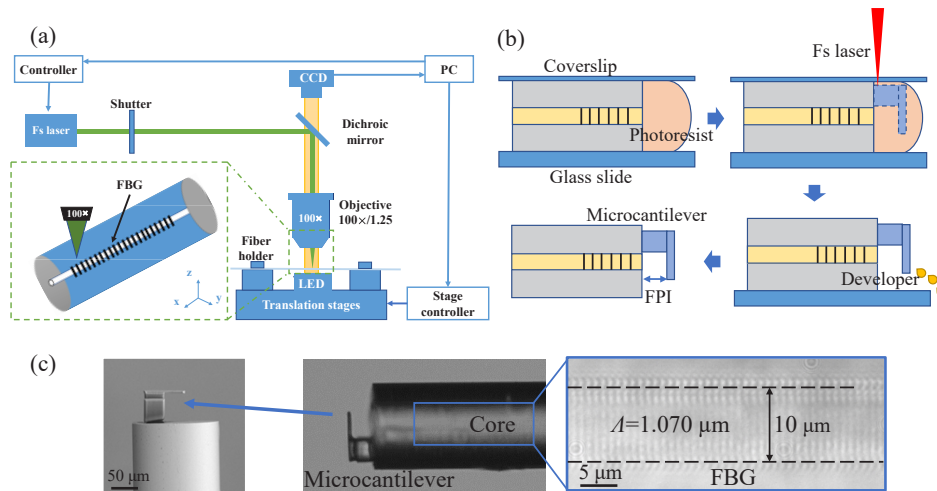


Fig. 2. (a) Schematic diagram of the fs-laser micromachining system for fabricating FBG, (b) process flow for fabricating the fiber-tip microcantilever, (c) micrographs of fabricated FBG-FPI sensor.

coverslip with its end face immersed in a PR drop. The polymerization fabrication was then performed on a 3D air bearing stage (Aerotech, UK) by fs laser with a pulse width of 250 fs, a central wavelength of 1026 nm and a pulse repetition rate of 200 kHz. An fs laser power of 2 mW and a scanning velocity of 300 μm/s was set to reduce the time cost. After polymerization, the unpolymerized PR was washed away by the developer solution of acetone and isopropyl alcohol (1:4, v/v). After washing and drying, the fiber-tip microcantilever was eventually fabricated. As shown in Fig. 2(c), the microcantilever was designed to be with a length of 30 μm, a width of 20 μm, and a thickness of 2 μm, respectively. The cavity length of the fiber-tip FPI was designed as 50 μm. There was an excellent parallelism between the fiber end face and the cantilever surfaces, which can enhance the intensity of reflection light and the detection sensitivity of the microcantilever deformation. After the two separated fabrication process, the FBG and FPI based on the fiber-tip microcantilever were integrated into the SMF.

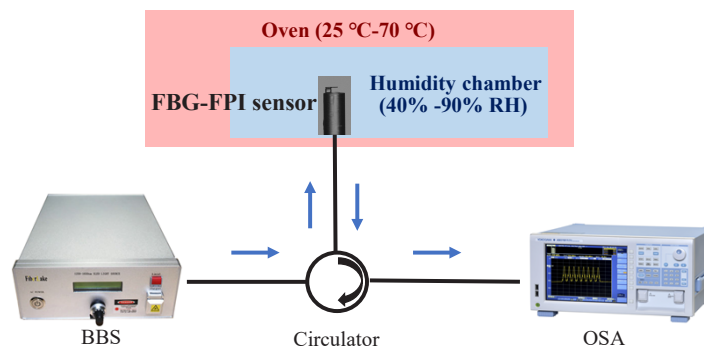


Fig. 3. Experimental setup of the FBG-FPI sensor for simultaneous measurement of temperature and humidity.

3.2. Experimental setup

Figure 3 shows the experimental setup of the proposed FBG-FPI sensor for simultaneous measurement of temperature and humidity. The input light from a broadband light source (BBS) (1250 to 1650 nm, Fiber Lake Co., Ltd., China) was coupled to the sensor through a circulator. The reflection spectra were then recorded by an optical spectrum analyzer (OSA, AQ6317C, Yokogawa, Japan) with a resolution of 0.02 nm.

4. Experiment and discussion

Figure 4 plots the superimposed reflection spectra of the FBG-FPI sensor, in which the resonance wavelength of the FBG was 1547.9 nm and the free spectral range of FP interference was 23.52 nm at 1555 nm.

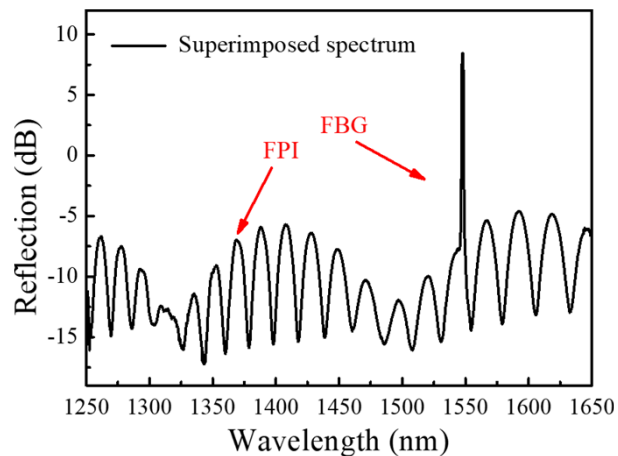


Fig. 4. Reflection spectra of the FBG-FPI sensor

During the humidity test, the sensor was placed in a homemade testing chamber with an accuracy of humidity control as $\pm 1\%$ RH. The humidity range was set from 40 to 90%RH, with the temperature controlled to be $25 \pm 0.1^\circ\text{C}$. During the measurement, the reflection spectra were monitored as the humidity increased in steps of 10%RH, and each humidity was maintained for at least 15 min to allow the sensor to reach the stable output. As shown in Fig. 5(a), there are two FPI-dips and an FBG-peak on interference spectra in the wavelength range from 1540 nm to 1600 nm. The FPI-dip wavelength (~ 1575 nm) showed a red shift of 8.78 nm with increasing humidity, while the FBG-peak wavelength almost did not shift. Figure 5(b) plots the zoomed-in reflection spectra illustrating the FBG-peak was almost constant as ~ 1547.9 nm regardless of the humidity change. Figure 5(c) shows the zoomed-in reflection spectra illustrating the 8.78 nm shift of FPI-dip wavelength (~ 1575 nm) as the humidity increased. As the relative humidity increased during the testing, the hygroscopic expansion of the microcantilever happened that could increase the thickness of microcantilever and decrease the refractive index of the polymer material of microcantilever, which eventually induced the optical path difference between reflected lights and resulted in the shift of the resonant wavelength of the reflected spectrum. For each humidity level, the error of the parallel measurements ($N=5$) for the corresponding FPI-dip wavelength shift was typically less than 10%. The linear fittings of humidity test results are shown in Fig. 5(d), in which the humidity sensitivity of FPI is as high as 0.348 nm/%RH ($R^2 = 0.974$). Such testing results suggested that the FPI sensing part demonstrated a high humidity sensitivity, while the FBG part was insensitive to humidity.

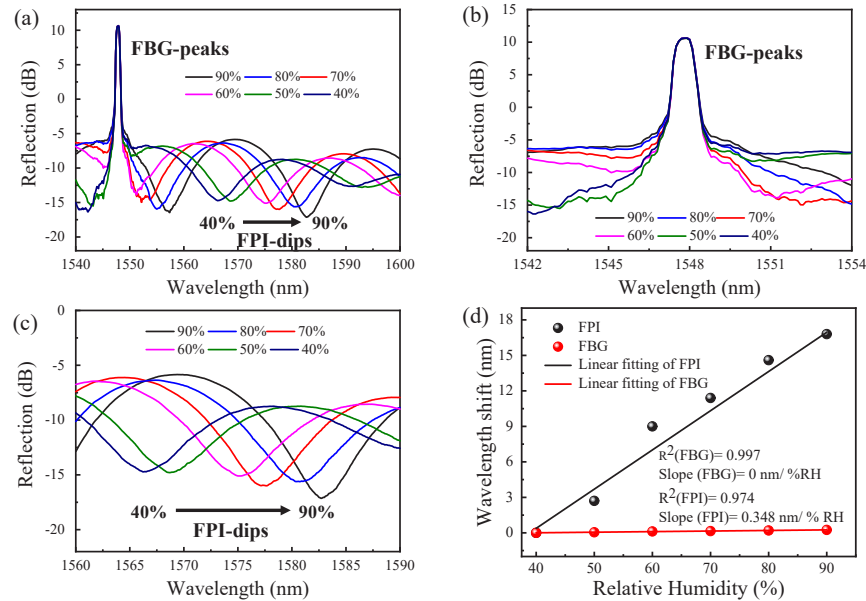


Fig. 5. Humidity responses of the FBG-FPI sensor: (a) reflection spectra of the FBG-FPI sensor with the increased humidity from 40 to 90%RH, (b) zoomed-in reflection spectra of the FBG-peak, (c) zoomed-in reflection spectra of the FPI-dip, (d) the linear fitting of humidity testing results.

In order to study the temperature response of the FBG-FPI sensor, the sensor was placed in an oven with a temperature controlling accuracy of 0.1 °C. The temperature was increased from 25 to 70 °C, and the reflection spectra were monitored as the temperature increased in steps of 5 °C, under normal humidity 40%RH. Each temperature was maintained for 15 min to allow the sensor to reach the stable output. As shown in Fig. 6(a), as the temperature increases from 25 to 70 °C, the FBG-peak shifts towards the long-wavelength direction, which is induced by the thermo-optic effect of the FBG. Figure 6(b) plots the zoomed-in reflection spectra illustrating the FBG-peak shifts 1.1 nm when the temperature changes. Figure 6(c) shows the zoomed-in reflection spectra illustrating the 4.7 nm shift of FPI-dip wavelength (~1575 nm) towards the short-wavelength direction, as the temperature increases. The mechanism is that, when the ambient temperature increases, the microcantilever is thermally expanded that inducing the increase of the FPI cavity length. The linear fitting of temperature testing results is shown in the Fig. 6(d), in which the temperature sensitivity of FPI is as high as -0.356 nm/°C ($R^2 = 0.991$), while the sensitivity of FBG is only 0.012 nm/°C ($R^2 = 0.988$).

To test the stability of the proposed sensor, additional humidity measurement lasting 24 hours has been conducted. By recording the FPI-dip wavelength at each humidity level (40%, 70% and 90%) every hour, the output response of the sensor as a function of time has been plotted in Fig. 7. The output FPI-dip wavelength turned out to be quite stable during the tested period, with the max data fluctuation of only 0.8 nm observed, corresponding to an uncertainty of 2.3%RH. Considering the measurement accuracy of the humidity testing chamber ($\pm 1\%$ RH), our proposed RH sensor showed an excellent stability.

During the real application, the ambient temperature and humidity usually change simultaneously. The wavelength shifts of the FPI-dip ($\Delta\lambda_{\text{FPI}}$) and FBG-peak ($\Delta\lambda_{\text{FBG}}$) can be expressed by

$$\Delta\lambda_{\text{FBG}} = A_1\Delta T + B_1\Delta RH \quad (3)$$

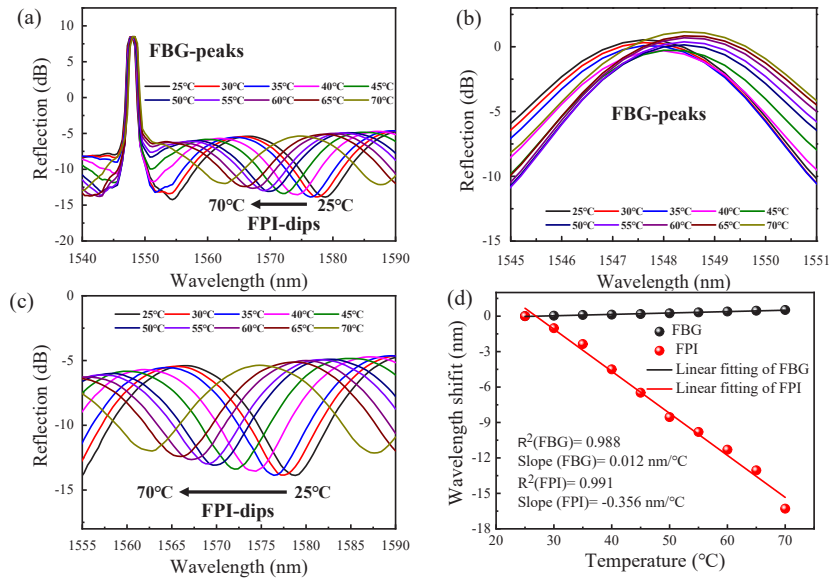


Fig. 6. Temperature responses of the FBG-FPI sensor: (a) reflection spectra of the FBG-FPI sensor with the increased temperature from 25 to 70°C, (b) zoomed-in reflection spectra of the FBG-peak, (c) zoomed-in reflection spectra of the FPI-dip, (d) the linear fitting of temperature testing results.

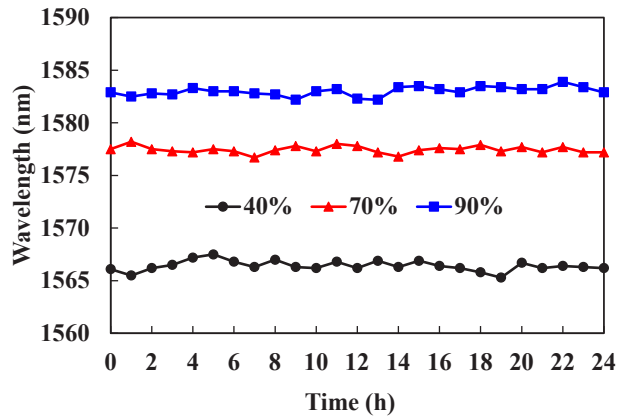


Fig. 7. Stability test result of the FBG-FPI sensor: the FPI-dip wavelength at each humidity level (40%, 70% and 90%) every hour recorded for 24 hours.

$$\Delta\lambda_{FPI} = A_2\Delta T + B_2\Delta RH \tag{4}$$

where A_1 and A_2 are the temperature sensitivities of the FBG and FPI, respectively; B_1 and B_2 are the humidity sensitivities of the FBG and FPI, respectively; ΔT is the temperature variation, and ΔRH is the humidity variation.

According to the temperature and humidity sensitivities of the sensor obtained by experiments, namely, $A_1 = 0.012 \text{ nm}/^\circ\text{C}$, $B_1 = 0 \text{ nm}/\%RH$, $A_2 = -0.356 \text{ nm}/^\circ\text{C}$, $B_2 = 0.348 \text{ nm}/\%RH$. Substituting these parameters into matrix, humidity and temperature variation as functions of FPI-dip ($\Delta\lambda_{FPI}$)

and FBG-peak ($\Delta\lambda_{FBG}$) could be obtained as:

$$\begin{bmatrix} \Delta\lambda_{FBG} \\ \Delta\lambda_{FPI} \end{bmatrix} = \begin{bmatrix} 0.012 & 0 \\ -0.356 & 0.348 \end{bmatrix} \begin{bmatrix} \Delta T \\ \Delta RH \end{bmatrix} \quad (5)$$

Eventually, the variation of temperature and humidity can be obtained by:

$$\begin{bmatrix} \Delta T \\ \Delta RH \end{bmatrix} = \begin{bmatrix} 0.012 & 0 \\ -0.356 & 0.348 \end{bmatrix}^{-1} \begin{bmatrix} \Delta\lambda_{FBG} \\ \Delta\lambda_{FPI} \end{bmatrix} \quad (6)$$

Therefore, this FBG-FPI sensor can be utilized to simultaneously monitor the humidity and ambient temperature using the sensitivity matrix. Thus, simultaneous measurement of temperature and humidity can be achieved.

In addition, the sensing performance of relevant works based on FBG and FPI (or other types of interferometers) for the simultaneous measurement of temperature and humidity has been summarized in Table 1. The sensor we reported has shown higher temperature and humidity sensitivity than that of other dual-parameter sensors based on dual FBGs or cascaded structures. With additional advantages of compact size and easy packaging, we anticipate the proposed hybrid fiber sensor has great potential in the applications involving in simultaneous measurement of temperature and humidity.

Table 1. Performance comparison of relevant fiber sensors for simultaneous measurement of temperature and humidity.^a

Fiber sensors	Temperature Sensitivity (pm/°C)		Humidity Sensitivity (pm/%RH)		References
	FBG	Interferometer	FBG	Interferometer	
Cascaded structure of FBG and FPI	9.98	NA (FPI)	NA	22.07 (FPI)	[22]
PCF-MZI and FBG	9.6	3.1 (MZI)	NA	-99.5 (MZI)	[23]
FBG-FP cavity	10.88	NA	NA	0.0682 dB (FPI)	[24]
Compact MZI and FPI	132(MZI)	72 (FPI)	370(MZI)	172 (FPI)	[6]
PMFFI and FBG	19.5	269.5 (PMFFI)	NA	54.5 (PMFFI)	[25]
Fiber-tip microcantilever cascading FBG	12	-356 (FPI)	NA	348 (FPI)	This work

^aMZI: Mach-Zehnder Interferometer; PMFF: Polymer Microcavity Fiber Fizeau Interferometer; PCF: Photonic Crystal Fiber

5. Conclusions

In this letter, we propose a high-sensitivity hybrid fiber sensor for simultaneous measurement of relative humidity and temperature. The sensor consisted of an FBG written in the core by fs-laser micromachining and an FPI based on the fiber-tip microcantilever fabricated by fs-laser induced TPP. The FPI sensing part achieved a humidity sensitivity of 0.348 nm/%RH and a temperature sensitivity of -0.356 nm/°C, respectively. The FBG part only showed a temperature sensitivity of 0.012 nm/°C and was turned out to be not sensitive to humidity. The ambient temperature can be measured by the FBG and further used as the temperature compensation to extract the exact humidity output of the FPI sensing part. Thus, a simultaneous measurement of temperature and humidity was achieved. According to the comparison of sensing performance with that of other relevant works, our proposed sensor was turned out to be with both higher temperature

and humidity sensitivity. Hence, we believe that this hybrid fiber sensor could offer an excellent solution for simultaneously measuring temperature and humidity in various applications

Funding. High-Talent Research Funding under Grant RC2022-001; Science, Technology and Innovation Commission of Shenzhen Municipality (JCYJ20190808161019406, JCYJ20200109114001806, RCYX20200714114524139); National Natural Science Foundation of China (62075136, 62101353, 62122057, 62205221).

Disclosures. The authors declare no conflicts of interest.

Data availability. Data underlying the results presented in this paper are not publicly available at this time but may be obtained from the authors upon reasonable request.

References

1. L. Alwis, T. Sun, and K. T. V. Grattan, "Fibre optic long period grating-based humidity sensor probe using a Michelson interferometric arrangement," *Sens. Actuators, B* **178**, 694–699 (2013).
2. S. Akita, H. Sasaki, K. Watanabe, and A. Seki, "A humidity sensor based on a hetero-core optical fiber," *Sens. Actuators, B* **147**(2), 385–391 (2010).
3. R.-Q. Lv, H.-K. Zheng, Y. Zhao, and Y.-F. Gu, "An optical fiber sensor for simultaneous measurement of flow rate and temperature in the pipeline," *Opt. Fiber Technol.* **45**, 313–318 (2018).
4. G. Yan, Y. Liang, H. Lee el, and S. He, "Novel Knob-integrated fiber Bragg grating sensor with polyvinyl alcohol coating for simultaneous relative humidity and temperature measurement," *Opt. Express* **23**(12), 15624–15634 (2015).
5. C. Wang, G. Yan, Z. Lian, X. Chen, S. Wu, and S. He, "Hybrid-cavity fabry-perot interferometer for multi-point relative humidity and temperature sensing," *Sens. Actuators, B* **255**, 1937–1944 (2018).
6. R.-J. Tong, Y. Zhao, H.-K. Zheng, and F. Xia, "Simultaneous measurement of temperature and relative humidity by compact Mach-Zehnder interferometer and Fabry-Perot interferometer," *Measurement* **155**, 107499 (2020).
7. L. Liang, H. Sun, N. Liu, H. Luo, T. Gang, Q. Rong, X. Qiao, and M. Hu, "High-sensitivity optical fiber relative humidity probe with temperature calibration ability," *Appl. Opt.* **57**(4), 872–876 (2018).
8. W. Bai, M. Yang, J. Dai, H. Yu, G. Wang, and C. Qi, "Novel polyimide coated fiber Bragg grating sensing network for relative humidity measurements," *Opt. Express* **24**(4), 3230–3237 (2016).
9. K. Guo, J. He, L. Shao, G. Xu, and Y. Wang, "Simultaneous Measurement of Strain and Temperature by a Sawtooth Stressor-Assisted Highly Birefringent Fiber Bragg Grating," *J. Lightwave Technol.* **38**(7), 2060–2066 (2020).
10. J. Luo, S. Liu, Y. Zhao, Y. Chen, K. Yang, K. Guo, J. He, C. Liao, and Y. Wang, "Phase-shifted fiber Bragg grating modulated by a hollow cavity for measuring gas pressure," *Opt. Lett.* **45**(2), 507–510 (2020).
11. W. Xu, W.-B. Huang, X.-G. Huang, and C.-Y. Yu, "A simple fiber-optic humidity sensor based on extrinsic Fabry-Perot cavity constructed by cellulose acetate butyrate film," *Opt. Fiber Technol.* **19**(6), 583–586 (2013).
12. P. Ji, M. Zhu, C. Liao, C. Zhao, K. Yang, C. Xiong, J. Han, C. Li, L. Zhang, Y. Liu, and Y. Wang, "In-Fiber Polymer Microdisk Resonator and Its Sensing Applications of Temperature and Humidity," *ACS Appl. Mater. Interfaces* **13**(40), 48119–48126 (2021).
13. J. Ascorbe, C. Sanz, J. M. Corres, F. J. Arregui, I. R. Matías, and S. C. Mukhopadhyay, "High sensitivity extrinsic Fabry-Pérot interferometer for humidity sensing," in *2015 9th International Conference on Sensing Technology (ICST)*, 2015, pp. 143–146.
14. J. Zhou, C. Liao, Y. Wang, G. Yin, X. Zhong, K. Yang, B. Sun, G. Wang, and Z. Li, "Simultaneous measurement of strain and temperature by employing fiber Mach-Zehnder interferometer," *Opt. Express* **22**(2), 1680–1686 (2014).
15. M. Zou, C. Liao, S. Liu, C. Xiong, C. Zhao, J. Zhao, Z. Gan, Y. Chen, K. Yang, D. Liu, Y. Wang, and Y. Wang, "Fiber-tip polymer clamped-beam probe for high-sensitivity nanoforce measurements," *Light: Sci. Appl.* **10**(1), 171 (2021).
16. C. Xiong, C. Liao, M. Zhu, Z. Gan, and Y. Wang, "Fiber-tip polymer microcantilever for hydrogen sensing," in *Asia Communications and Photonics Conference/International Conference on Information Photonics and Optical Communications 2020 (ACP/IPOC)*, Beijing, 2020, p. S31.1.
17. P. K. Wong, Y. K. Lee, and C. M. Ho, "Deformation of DNA molecules by hydrodynamic focusing," *J. Fluid Mech.* **497**, S002211200300658X55 (2003).
18. C. Zhao, D. Liu, Z. Cai, B. Du, M. Zou, S. Tang, B. Li, C. Xiong, P. Ji, L. Zhang, Y. Gong, G. Xu, C. Liao, and Y. Wang, "A Wearable Breath Sensor Based on Fiber-Tip Microcantilever," *Biosensors* **12**(3), 168 (2022).
19. C. R. Liao, Y. Wang, D. N. Wang, and M. W. Yang, "Fiber In-Line Mach-Zehnder Interferometer Embedded in FBG for Simultaneous Refractive Index and Temperature Measurement," *IEEE Photonics Technol. Lett.* **22**(22), 1686–1688 (2010).
20. J. Luo, S. Liu, P. Chen, S. Lu, Q. Zhang, Y. Chen, B. Du, J. Tang, J. He, C. Liao, and Y. Wang, "Fiber optic hydrogen sensor based on a Fabry-Perot interferometer with a fiber Bragg grating and a nanofilm," *Lab Chip* **21**(9), 1752–1758 (2021).
21. C. Li, C. Liao, J. Wang, Z. Li, Y. Wang, J. He, Z. Bai, and Y. Wang, "Femtosecond laser microprinting of a polymer fiber Bragg grating for high-sensitivity temperature measurements," *Opt. Lett.* **43**(14), 3409–3412 (2018).
22. Y. Wang, Q. Huang, W. Zhu, and M. Yang, "Simultaneous Measurement of Temperature and Relative Humidity Based on FBG and FP Interferometer," *IEEE Photonics Technol. Lett.* **30**(9), 833–836 (2018).

23. S. Zhang, X. Dong, T. Li, C. C. Chan, and P. P. Shum, "Simultaneous measurement of relative humidity and temperature with PCF-MZI cascaded by fiber Bragg grating," *Opt. Commun.* **303**, 42–45 (2013).
24. Y. Qi, C. Jia, L. Tang, M. Wang, Z. Liu, and Y. Liu, "Simultaneous measurement of temperature and humidity based on FBG-FP cavity," *Opt. Commun.* **452**, 25–30 (2019).
25. C.-L. Lee, Y.-W. You, J.-H. Dai, J.-M. Hsu, and J.-S. Horng, "Hygroscopic polymer microcavity fiber Fizeau interferometer incorporating a fiber Bragg grating for simultaneously sensing humidity and temperature," *Sens. Actuators, B* **222**, 339–346 (2016).